The first-order Raman spectra of OsO_2

2003 J. Phys.: Condens. Matter 15 1487

(http://iopscience.iop.org/0953-8984/15/9/312)

INSTITUTE OF PHYSICS PUBLISHING JOURNAL OF PHYSICS: CONDENSED MATTER

J. Phys.: Condens. Matter **15** (2003) 1487–1494 PII: S0953-8984(03)55681-8

The first-order Raman spectra of OsO_2

P C Yen[1], R S Chen[1], Y S Huang[1,4], C T Chia[2], R H Chen[2] and K K Tiong[3]

[1] Department of Electronic Engineering, National Taiwan University of Science and Technology, Taipei 106, Taiwan, Republic of China
[2] Department of Physics, National Taiwan Normal University, Taipei 117, Taiwan, Republic of China
[3] Department of Electrical Engineering, National Taiwan Ocean University, Keelung 202, Taiwan, Republic of China

Received 6 November 2002, in final form 22 January 2003
Published 24 February 2003
Online at stacks.iop.org/JPhysCM/15/1487

Abstract

The first-order Raman spectra of the transition metal dioxide OsO_2 with tetragonal rutile structure have been measured at room temperature. A linearly polarized argon laser light source and completely oriented single-crystal samples have made possible unambiguous determination of the four allowed Raman-active phonon modes. Comparison is made with results for other rutile materials.

1. Introduction

The family of transition metal dioxide compounds with rutile-type structure possesses an interesting variety of electrical and magnetic properties [1]. Conductive transition metal dioxides with rutile-type structure show potential applications in substituting for the metals currently used in conductive lines which serve to connect components of semiconductor and electrode materials in ferroelectric memory devices [2–4]. Osmium dioxide, OsO_2, belongs to this family of compounds; little is known of its fundamental properties. This may be due in part to the highly toxic nature of the readily formed and volatile tetroxide of the material [5].

This report presents the first-order Raman spectra of OsO_2. To the best of our knowledge only one such report on the phonon frequencies of the four Raman-active modes in OsO_2 exists [6]. The existing literature merely lists a Raman spectrum from a small crystal of OsO_2, oriented so as to display all four Raman-active lines. In the present study, the group symmetry restraints of the Raman-active phonons and the Raman selection rules are discussed. The results are then utilized to classify the experimentally observed polarized Raman spectra of the four phonon modes. Comparisons are made with results for other metal dioxide [7–13] and metal fluoride [10, 14] compounds, which possess similar rutile-type structure.

[4] Author to whom any correspondence should be addressed.

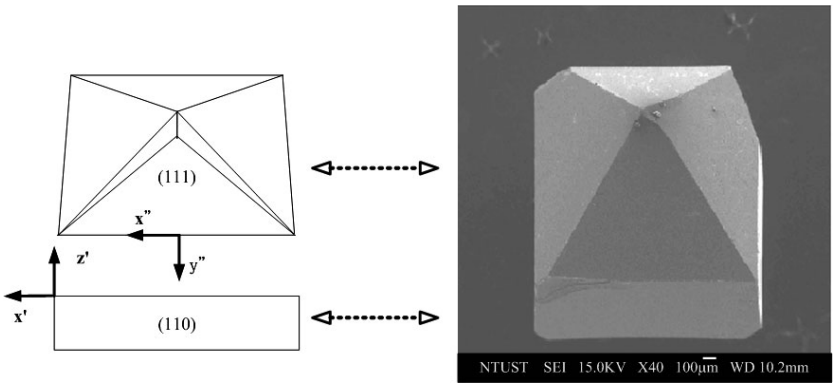

Figure 1. A photograph of an OsO_2 crystal showing the (110) and (111) planes together with the polarization axes.

2. Experimental details

Single crystals of OsO_2 with well-developed faces were grown in our laboratory by the chemical transport method [15]. OsO_2 was grown by the oxidation of high-purity osmium with excess $NaClO_3$ or $NaBrO_3$ in an evacuated, sealed silica tube. The volume of the tube was about 100 cm^3 after sealing, and the excess $NaClO_3$ or $NaBrO_3$ was sufficient to complete oxidation of Os to OsO_2. The processes of $NaClO_3$ or $NaBrO_3$ decomposition and Os oxidation were accomplished simultaneously by slowly heating the silica tube and its contents to 300 °C over 48 h and subsequently firing at 650 °C for an additional 48 h. This treatment resulted in an apparent complete decomposition of the chlorate or bromate with the formation of golden OsO_2 powder in one end of the tube. The tube was then transferred to a horizontal furnace and positioned so as to provide a temperature gradient along the length of the tube, which is about 20 cm long. The charge of OsO_2 in one end was maintained at 920 °C, and the opposite end of the tube was held at 900 °C for 240 h. The transported crystals were about 3–5 mm across a polyhedral face. The x-ray powder diffraction analysis was performed to ascertain that tetragonal rutile structure had been obtained. The crystals were x-ray pre-oriented with respect to the directions and polarizations of the incident and scattered light. A representative crystal showing the as-grown (110) and (111) planes together with the prescribed polarization configurations is illustrated in figure 1.

Raman measurements were made on as-grown (110) and (111) faces in the backscattering geometry utilizing a DILOR XY-800 triple-grating Raman spectrometer equipped with a liquid-nitrogen-cooled CCD and an OLYMPUS BH-2 microscope. The 5145 Å line of an argon ion laser was used as the excitation source, and was focused on the sample surface with a 100× objective. The focusing spot size is about 1 μm in diameter and the laser power density is estimated to be about 1 W cm^{-2}. Prior to the measurement, the system was calibrated by means of the 520 cm^{-1} Raman peak of a Si single crystal. The spectra exhibited approximately a 0.5 cm^{-1} resolution with the slit width of 30 μm. For frequency less than 250 cm^{-1}, an argon purge was used to suppress the N_2 lines.

3. Symmetry analysis

OsO_2 has the tetragonal rutile structure belonging to the space group D_{4h}^{14} with two OsO_2 molecules per unit cell as shown in figure 2. The cations are located at sites with D_{2h} symmetry

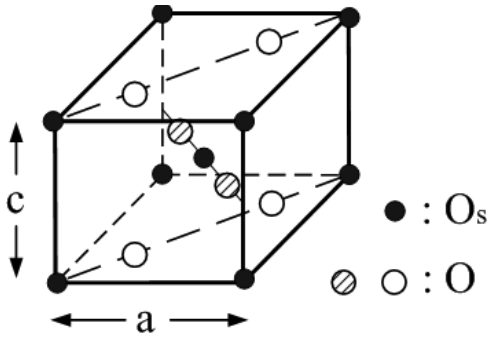

Figure 2. A schematic representation for a unit cell of OsO_2.

and the anions occupy sites with C_{2v} symmetry. The Os ions are surrounded by six oxygen ions at the corners of a slightly distorted octahedron, while the three Os ions coordinating each of the oxygen ions lie in a plane at the corners of a nearly equilateral triangle. There are four Raman-active modes with symmetries A_{1g}, B_{1g}, B_{2g}, and E_g [15]. The first three are singlets and the last is a doublet.

Corresponding to each Raman-active mode, there is a scattering tensor α having a distinctive symmetry. For the four allowed Raman transitions in materials of D_{4h}^{14} space group, these tensors have the form [16]

$$\alpha(A_{1g}) = \begin{pmatrix} a & 0 & 0 \\ 0 & a & 0 \\ 0 & 0 & b \end{pmatrix}, \qquad \alpha(B_{1g}) = \begin{pmatrix} c & 0 & 0 \\ 0 & -c & 0 \\ 0 & 0 & 0 \end{pmatrix}, \qquad \alpha(B_{2g}) = \begin{pmatrix} 0 & d & 0 \\ d & 0 & 0 \\ 0 & 0 & 0 \end{pmatrix}$$
$$\alpha(E_g) = \begin{pmatrix} 0 & 0 & 0 \\ 0 & 0 & e \\ 0 & e & 0 \end{pmatrix} \qquad \text{and} \qquad \begin{pmatrix} 0 & 0 & e \\ 0 & 0 & 0 \\ e & 0 & 0 \end{pmatrix}. \tag{1}$$

The displacements of atoms associated with the four Raman-active vibrations are shown in figure 3 [9]. To examine experimentally a given component α_{ij}, the geometry is arranged such that the incident light is polarized in the i-direction while only the scattered light of j-polarization is observed.

A full classification of the four Raman-active modes may be accomplished as follows. The geometric configurations for the various axes used in this experiment are denoted as

$$\begin{aligned} x' &= \frac{1}{\sqrt{2}}(1\bar{1}0) & x'' &= \frac{1}{\sqrt{2}}(1\bar{1}0) \\ y' &= \frac{1}{\sqrt{2}}(110) & y'' &= \frac{1}{\sqrt{6}}(11\bar{2}) \\ z' &= (001) & z'' &= \frac{1}{\sqrt{3}}(111). \end{aligned} \tag{2}$$

The expressions for the relative Raman intensities correlating to various $|\alpha_{ij}|^2$ for the two different crystal orientations along (110) and (111) faces in the backscattering configurations are listed in table 1. The results show that the B_{1g} mode is forbidden for all configurations for scattering from the (110) face and is allowed only for the $\alpha_{x''y''}$-configuration from the (111) face. The E_g mode is allowed for $\alpha_{x'z'}$-, $\alpha_{x''y''}$-, and $\alpha_{y''y''}$-configurations, while the allowed configurations for the A_{1g} mode are $\alpha_{x'x'}$, $\alpha_{z'z'}$, $\alpha_{x''x''}$, and $\alpha_{y''y''}$. The B_{2g} mode is allowed for $\alpha_{x'x'}$-, $\alpha_{x''x''}$-, and $\alpha_{y''y''}$-configurations.

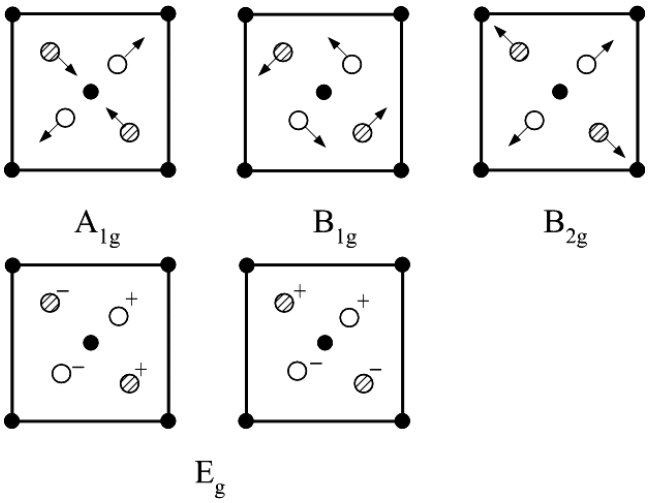

Figure 3. The displacements of atoms of OsO_2, viewed along the *c*-axis, associated with the four first-order Raman-active modes of rutile structure.

Table 1. Relative Raman intensities for the B_{1g}, E_g, A_{1g}, and B_{2g} phonon modes for the various polarization configurations used in this experiment.

	Phonon mode			
Polarization configuration	B_{1g}	E_g	A_{1g}	B_{2g}
			(110) face	
$\alpha_{x'x'}$	0	0	a^2	d^2
$\alpha_{x'z'}$	0	e^2	0	0
$\alpha_{z'z'}$	0	0	b^2	0
			(111) face	
$\alpha_{x''x''}$	0	0	a^2	d^2
$\alpha_{x''y''}$	$(1/3)c^2$	$(2/3)e^2$	0	0
$\alpha_{y''y''}$	0	$(8/9)e^2$	$(1/9)(a+2b)^2$	$(1/9)d^2$

4. Results and discussion

Plotted in figures 4(a)–(c) are the Raman spectra observed for scattering from the as-grown (110) surface of single-crystal OsO_2 for the cases of $\alpha_{x'x'}$-, $\alpha_{x'z'}$-, and $\alpha_{z'z'}$-configurations, respectively. Figure 4(a) shows two Raman peaks at 685 and 726 cm^{-1} whereas figures 4(b) and (c) show only one peak each at 544 and 685 cm^{-1}, respectively. Mode assignment with the aid of table 1 shows that these features correspond to the E_g mode (544 cm^{-1}), the A_{1g} mode (685 cm^{-1}), and the B_{2g} phonon (726 cm^{-1}). Our identification of the peak positions of the three lines agreed extremely well with that of [6], which is so far the only report on the material.

In figures 5(a)–(c) we display the Raman spectra seen for scattering from the (111) face for the polarization arrangements $\alpha_{x''x''}$, $\alpha_{x''y''}$, and $\alpha_{y''y''}$, respectively. Note that in figure 5(b), in addition to a strong peak at 544 cm^{-1}, a very sharp weak feature at 184 cm^{-1} is observed. This is the B_{1g} phonon mode and the peak position agrees very well with that of [6] where it is determined as being at 187 cm^{-1}. This is the only configuration where the B_{1g} line is

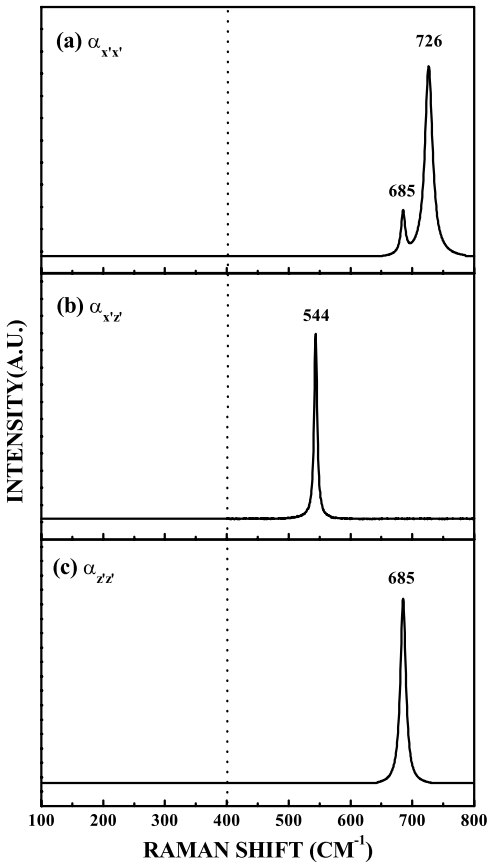

Figure 4. The Raman spectra observed for scattering from the (110) surface of single-crystal OsO_2. (a) The $\alpha_{x'x'}$-configuration showing the A_{1g} and B_{2g} phonons at 685 and 726 cm^{-1}, respectively. (b) The $\alpha_{x'z'}$-configuration showing the E_g phonon at 544 cm^{-1}. (c) The $\alpha_{z'z'}$-configuration showing the A_{1g} phonon at 685 cm^{-1}.

allowed (see table 1). The polarization configurations of the other three Raman signatures at locations 544, 685, and 726 cm^{-1} lead to a consistent symmetry assignment of these structures as indicated by table 1 and with that given by figures 4(a)–(c). It is also worth noting that the relative intensity ratios of B_{2g} to A_{1g} modes for $\alpha_{x'x'}$- and $\alpha_{x''x''}$-configurations are consistent with that given by table 1, where $I(B_{2g})/I(A_{1g}) = d^2/a^2 \approx 3.4$.

As shown in figures 4 and 5, the Raman spectra of OsO_2 exhibit strong lines of A_{1g}, E_g symmetries, a high-frequency line of B_{2g} symmetry, and a very sharp and weak low-frequency B_{1g} mode. A careful search for the B_{1g} mode is necessary, since the intensity of this mode is smaller than that of the E_g mode by a factor of 50 or more. The frequency and symmetry assignments for the four Raman-active phonons of OsO_2 are listed in table 2. For completeness and comparison, the table also summarizes the previously reported results for a number of other metal dioxides (OsO_2 [6], RuO_2 [7, 8], IrO_2 [9], TiO_2 [10], SnO_2 [11], and CrO_2 [12]), GeO_2 [13], and metal fluorides (MgF_2 [10], ZnF_2 [10], FeF_2 [10], MnF_2 [10], and CoF_2 [14]) with the rutile structure.

The Raman spectra of OsO_2 are quite sharp, with very little background. The observed full width at half-maximum (FWHM) at room temperature is about 2.4, 6.2, 8.3, and 14.4 cm^{-1}

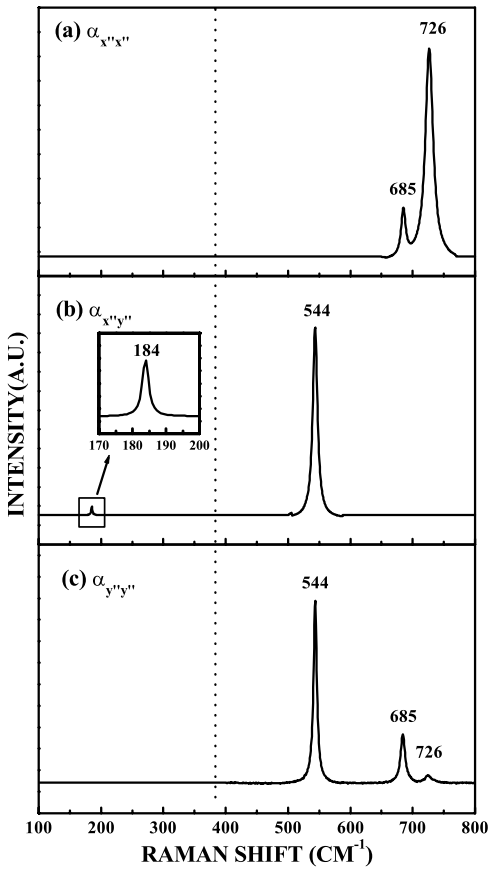

Figure 5. The Raman spectra observed for scattering from the (111) surface of single-crystal OsO_2. (a) The $\alpha_{x''x''}$-configuration showing the A_{1g} and B_{2g} phonons at 685 and 726 cm^{-1}, respectively. (b) The $\alpha_{x''y''}$-configuration showing the B_{1g} and E_g phonons at 184 and 544 cm^{-1}, respectively. (c) The $\alpha_{y''y''}$-configuration showing the E_g, A_{1g}, and B_{2g} phonons at 544, 685, and 726 cm^{-1}, respectively.

for B_{1g}, A_{1g}, E_g, and B_{2g} modes, respectively. These values are comparable to those for the insulating rutile materials and unlike those for metallic VO_2 [18] (rutile structure), for which only a strong, broad band near 550 cm^{-1} has been observed. It is also most appropriate to compare the Raman spectra of OsO_2 to those of the isostructural dioxide compounds of Ir, Ru, and Cr. The B_{2g} mode of these metal dioxides is comparatively soft as compared to the corresponding phonon modes of the insulating metal oxides TiO_2 [10] and SnO_2 [11]. The relative intensities of the B_{2g} mode in the metallic materials OsO_2 (see figures 4 and 5), IrO_2, RuO_2, and CrO_2 are considerably greater compared to those for the transparent rutile materials [9, 10, 12]. Srivastava and Chase [12] have attributed this behaviour in CrO_2 to a plasma-edge-induced resonance enhancement. In the B_{2g} mode, all of the nearest-neighbour oxygen atoms move toward one cation and away from the other inequivalent cation in the unit cell. This mode is likely to be resonance enhanced by the plasma edge present in the metallic-like oxides because of the charge density fluctuations produced near the cation sites by such oxygen displacements. Table 2 shows that OsO_2 has the hardest B_{1g} mode of all the rutile materials investigated to date. The similarity of the Raman-active phonons for OsO_2 and

Table 2. Raman-active phonons in a number of materials with the rutile structure.

	Mode (cm^{-1})			
Material	B_{1g}	E_g	A_{1g}	B_{2g}
OsO_2[a]	184	544	685	726
OsO_2 [6]	187	545	685	727
RuO_2 [7]	97	528	646	716
RuO_2 [8]	165	526	646	715
IrO_2 [9]	145	561	752	728
TiO_2 [10]	143	447	612	826
SnO_2 [11]	123	475	634	776
CrO_2 [12]	—	470	575	700
GeO_2 [13]	97	680	702	870
MgF_2 [10]	92	295	410	515
ZnF_2 [10]	70	253	350	522
FeF_2 [10]	73	257	340	496
MnF_2 [10]	61	247	341	476
CoF_2[b] [14]	68	246	366	494

[a] Present work.
[b] Measured at 77 K.

RuO_2 is quite striking—except for the value for the soft B_{1g} mode from [7]. The two reports, references [7] and [8], on RuO_2 differed significantly only as regards the location of the soft B_{1g} mode (97 cm^{-1} for [7] and 165 cm^{-1} for [8]). It is speculated that such a discrepancy may result from slight oxygen deficiency [8] (and references within) in the samples used in [7]. In any case, the higher frequency value of 165 cm^{-1} seems to be more consistent with the values for B_{1g} modes for the other metal dioxides with rutile structure [9–11] and most significantly with the value of 184 cm^{-1} (187 cm^{-1} from [6]) for OsO_2. The reason for the close similarity is that OsO_2 and RuO_2 are structurally identical, with four d electrons per cation. The relatively weak oscillator strength for the B_{1g} mode, as shown consistently by our results and the previous reports [6–9], indicates an inherent physical character for rutile structure crystals belonging to the D_{4h}^{14} space group.

5. Summary

In summary, the polarized first-order Raman spectra have been measured at room temperature for single crystals of metallic OsO_2. The four Raman-active phonons predicted by group theory have been observed and classified. Comparison is made with results for other rutile materials. The B_{2g} mode is softer compared to the corresponding phonons in the insulating material oxides, while OsO_2 shows the hardest B_{1g} mode of all the rutile materials investigated to date.

Acknowledgment

The authors acknowledge the support of the National Science Council of the Republic of China.

References

[1] Mattheiss L F 1976 *Phys. Rev.* B **13** 2433
[2] Kolawa E, So F C T, Pan E T S and Nicolet M A 1987 *Appl. Phys. Lett.* **50** 854

[3] Nakamura T, Nakao Y, Kamisawa A and Takasu H 1994 *Appl. Phys. Lett.* **65** 1522
[4] Al-Shareef H N, Bellur K R, Kingon A I and Auciell O 1995 *Appl. Phys. Lett.* **66** 239
[5] Balfour W J and Ram R S 1984 *J. Mol. Spectrosc.* **105** 360
[6] Weber W H and Merlin R 2000 *Raman Scattering in Materials Science* (Berlin: Springer)
[7] Huang Y S and Pollak F H 1982 *Solid State Commun.* **43** 921
[8] Rosenblum S S, Weber W H and Chamberland B L 1997 *Phys. Rev.* B **56** 529
[9] Huang Y S, Lin S S, Huang C R, Lee M C, Dann T E and Chien F Z 1989 *Solid State Commun.* **70** 517
[10] Porto S P S, Fleury P A and Damen T C 1967 *Phys. Rev.* **154** 522
[11] Peercy P S and Morosin B 1973 *Phys. Rev.* B **7** 2779
[12] Srivastava R and Chase L L 1972 *Solid State Commun.* **11** 349
[13] Scott J F 1970 *Phys. Rev.* B **1** 3488
[14] MacFarlane R M and Ushioda S 1970 *Solid State Commun.* **8** 1081
[15] Schäfer H 1964 *Chemical Transport Reactions* (New York: Academic)
[16] Loudon R 1964 *Adv. Phys.* **13** 423
[17] Loudon R 1963 *Proc. Phys. Soc.* **82** 393
[18] Srivastava R and Chase L L 1971 *Phys. Rev. Lett.* **27** 727